Aalborg Universitet

AALBORG UNIVERSITY
DENMARK

Experimental damping assessment of a full scale offshore mono bucket foundation

Gres, Szymon; Fejerskov, Morten; Ibsen, Lars Bo; Damkilde, Lars

Experimental damping assessment of a full scale offshore Mono Bucket foundation

S. Gres [1,2,3]**, M. Fejerskov** [2]**, L.B. Ibsen** [1]**, L. Damkilde** [1]

[1] Aalborg University, Department of Civil and Structural Engineering,
Sofiendalsvej 9-11, Aalborg, Denmark
[2] Universal Foundation A/S,
Langerak 17.1, Aalborg, Denmark
[3] e-mail: **sg@civil.aau.dk**

Abstract

This paper quantifies the system damping of a offshore meteorological mast supported by a Mono Bucket foundation based on a long-term experimental campaign. The structure is located at Dogger Bank west, North Sea, and equipped with a measurement system monitoring acceleration, strain, inclination and sea surface elevation. Natural frequencies and corresponding damping ratios are assessed using different operational modal analysis techniques, enhanced frequency domain decomposition and stochastic subspace identification. Application and results from both methods are compared and discussed. Research shows that the total damping ratio of the lowest eigenmode is normally distributed with mean value of 1.11% of critical damping. Linear correlation between the damping ratio and the significant wave height is observed.

1 Introduction

The high demand for clean energy production has led to a great development in the field of offshore and onshore wind energy in the past years. Offshore wind generates higher design, installation and maintenance costs compared to onshore wind, however it is more effective in the power production due to the higher and more constant wind speeds and no limitations regarding the turbine sizes on the offshore sites. Despite the strive to deploy the increasingly larger turbines in the deeper waters with challenging soil conditions, the most frequently used support for the offshore wind turbines is still a monopile foundation. The size of the modern monopiles reaches up to a 7.8 m in diameter and a weight of 1300 tons, which generate significant costs as well as challenges during the production. The global imperative to reduce the cost of offshore wind has resulted in a new support concept based on the suction technique - Mono Bucket and Suction Bucket Jacket foundations.

The Mono Bucket (MB) originates from the oil and gas suction anchors [1]. The concept merges the advantages of the suction technology, the bearing resistance of gravity based foundation and the skirt resistance of the monopiles, resulting in a foundation which is light and easy to install/decommission. Hence the MB is a relatively light offshore support with a high stiffness in the embedded part [1] the fatigue due to wind and wave loads is the design driver for the foundation. The complex nature of the offshore loads that dynamically interact with the structural system pose a challenge towards the designers and call for the close identification of the parameters that influence the overall design. As an example, results from [2] state that for a offshore monopile the increase in the damping ratio by 50% results in the decrease of the fatigue loads by 20%. This substantial decrease in the loads justifies the interest of the industry towards accurate assessment of the dynamic properties of the system and supports the idea behind full scale offshore experimental campaigns.

The damping of the offshore system, or so-called offshore damping, consists of aerodynamic, hydrodynamic, soil and structural damping. The aerodynamic damping reflects the motion of the tower counteracted by the increase/decrease of the aerodynamic force from the turbine blades [3] and is a major source of damping for the operating turbine.

The hydrodynamic damping is the sum of two contributions - wave radiation and viscous damping of the fluid. Both components are proportional to the relative velocity between the structure and the water. The hydrodynamic damping ratios recommended by the Germanischer Lloyd, GL, in [4] are 0.11% and 0.15% for the radiation and the viscous damping respectively.

The soil damping is divided in geometric, material and pore pressure components. The geometric damping describes the wave radiation into the soil volume and is neglected for frequencies below 1 Hz [5]. The pore pressure part is related to the permeability and the water dissipation in the pores of the soil. Hysteretic material damping of the soil, as well as the steel, is described as an absorption of the motion due to the internal friction of the material. For the piled supports GL recommends the soil damping ratios between 0.53%-0.88% and the steel damping between 0.2%-0.3% [4].

The best estimates for the overall added offshore damping subtracted with the aerodynamic damping, are stated as 0.9% and 1.2% depending on the simulation type [4].

The offshore damping is not as extensively researched topic for the MB as for the monopile supports. A single experimental campaign regarding the cross-wind damping of Vestas V90-3MW offshore wind turbine supported by the prototype MB foundation was presented in [6]. The results provided the correlation between the structural accelerations and the soil damping with the maximum damping ratio of 0.6% for an acceleration level of 2.1 $\frac{m}{s^2}$. Due to the fact that the tests were conducted in near shore laboratory the site conditions were not fully reflecting the offshore environment what influences the components of the system damping.

The main purpose of this study is to determine the long term dynamic characteristics, eigenfrequencies and damping ratios, of the offshore meteorological mast at Dogger Bank (DB) wind farm supported by the MB foundation. For this purpose the time and frequency domain OMA techniques are applied on the long-term operational data from the structure. The results are correlated with the measured sea states and compared with existing publications. The single components of system damping ratio are separated. A database of the damping ratios for the analyzed location is created as a reference for future designs.

2 Structure and site conditions

The meteorological mast is located in the west of the site and is one of the two masts supported by the MB installed at DB. On-site photo from the installation vessel is presented in Figure 1.

2.1 Structure

The MB is a modular welded steel foundation, divided into a shaft, webs, lid, and skirt modules. The webs and the shaft form a main frame of the foundation. The lid and the skirt create a horizontal and vertical base respectively. The MB is installed by the combination of self-weight and applied suction. The base is designed with 9 radial webs, diameter of 15 m, 7.5 m skirt length and 42.5 m shaft length, illustrated in Figure 2. Three so-called clay chambers assist and provide active inclination control during the installation process.

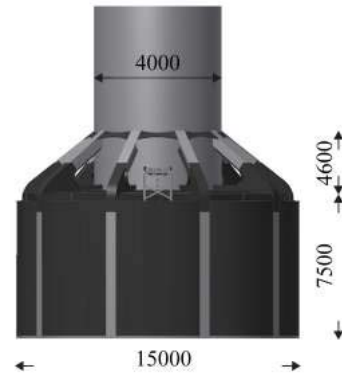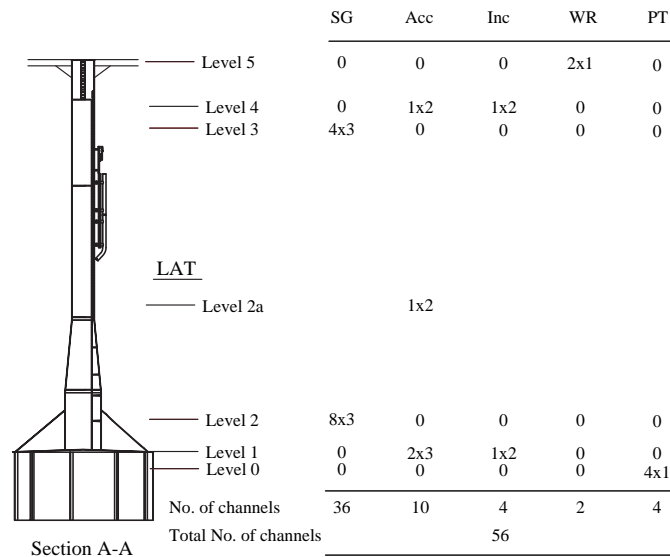Figure 1: The Mono Bucket foundations for the masts at DB.

Figure 2: The geometry of the foundation. All dimensions in millimeters.

The platform is connected to the shaft of the MB by 4 radial girders. A three legged meteorological mast of 91.5 m is bolted to the platform. The primary steel of the MB weights 276 tons. The secondary steel consists of the boat landing attached to the south side of shaft. Cathodic protection attached to the cylinder below the platform is used for corrosion protection, see Figure 1.

2.2 Structural monitoring

The structural monitoring sensor system setup consists of the accelerometers (Acc), inclinometers (Inc), strain gauges (SG), wave gauges (WR) and pressure transducers (PT). The configuration of all the sensors is presented in Figure 3.

	SG	Acc	Inc	WR	PT
Level 5	0	0	0	2x1	0
Level 4	0	1x2	1x2	0	0
Level 3	4x3	0	0	0	0
Level 2a		1x2			
Level 2	8x3	0	0	0	0
Level 1	0	2x3	1x2	0	0
Level 0	0	0	0	0	4x1
No. of channels	36	10	4	2	4
Total No. of channels			56		

Section A-A

LAT

number of gauge x direction: 1x2 = 1 gauge with x and y directions
1x3 = 1 gauge with x,y and z directions

Figure 3: Arrangement of the structural monitoring system at the DB mast.

This study uses the accelerations and the surface elevations measurements to determine the relation between the modal characteristics of the structure and the environmental conditions. Accelerations are measured by

the *AS-5TG* bi-axial and tri-axial accelerometers on the top of the shaft and the lid of the foundation. Two *VegaPlus 61* wave radars measuring the instantaneous sea surface elevations are installed on the platform of the mast. Data is collected by the mobile, self sustainable SOMAT eDAQ acquisition system and saved on the industrial PC located in the shaft of the foundation.

2.3   Site conditions

Dogger Bank west is located at North Sea, 150 km to the east coast of UK. The water depth for the considered position is 24.8 m. The soil profile based on the in-situ testing consists of layers of dense sand and stiff clay and is listed in Table 1.

Depth [m]	Soil type	E_{50} [MPa]	E_{ur} [MPa]	ϕ'	c'_{ref} [kPa]
2.0	Sand, very dense	90.8	27.2	-	42.1
5.0	Clay, soft	6.3	15	40	-
5.5	Sand, very dense	90.8	27.2	-	42.1
13.6	Clay, firm	11.9	28.5	40	-
26.0	Clay, stiff	15.6	37.5	40	-

Table 1: Soil parameters based on the CPT.

E_{50}, E_{ur}, ϕ' and c'_{ref} are the secant modulus in drained triaxial test, the unloading/reloading modulus, the friction angle and the cohesion of the soil respectively. Regarding scour, bathymetry survey using the multi-beam echo sounder conducted in October 2014 concluded local 1m scour hole.

3   Applied system identification techniques

The dynamic properties of the meteorological mast is highly affected by the magnitude of ambient excitations. The convenient method to determine the modal parameters of such structure is to use output only system identification techniques with the responses analyzed for the similar loading conditions. In this paper Enhanced Frequency Domain Decomposition [7] (EEFD) and Stochastic Subspace Identification [8] (SSI) techniques are applied.

3.1   Enhanced Frequency Domain Decomposition

The EFDD, proposed in [7], is a modification of the Frequency Domain Decomposition technique that originates from a basic frequency domain approach. Both methods utilize that any lightly damped mode influence the response of the structure in the vicinity of its natural frequency. The difference is that (E)FDD uses singular value decomposition (SVD), of the response power spectral density matrices (PSD). The EFDD method was chosen and implemented in MATLAB. Below is a general description of the method.

The dynamic response of a linear system can be represented as a sum of a product of the mode shapes, ϕ_i, and the modal coordinates q_i. The covariance function of a system response yields (1), [7].

$$C_{yy}(\tau) = E[\{y(t+\tau)\}\{y(t)\}^H] = E[[\phi]\{q(t+\tau)\}\{q(t)\}^H[\phi]^H] = [\phi][C_{qq}(\tau)][\phi]^H \qquad (1)$$

where subscript ^{H} denotes a complex conjugate and transpose. Auto and cross spectral densities are calculated using a Welch averaged periodogram with the 50% signal overlapping and Hanning windowing (2), [9].

$$G_{yy}(f) = [\phi][G_{qq}(f)][\phi]^H \qquad (2)$$

The key procedure in EFDD is to decompose the PSD matrices using the SVD and describe them as a set of the spectral density functions each corresponding to a SDOF system (3) illustrated in Figure 4.

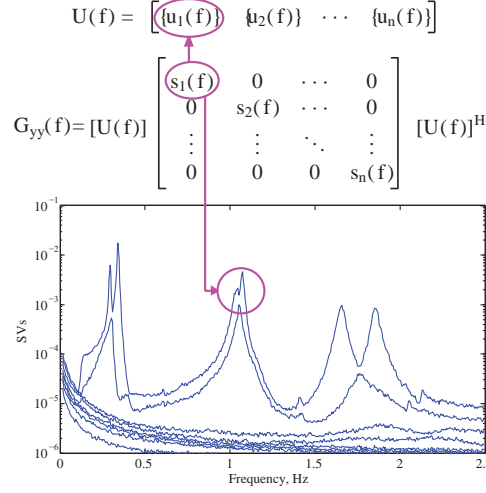$$G_{yy}(f) = [U(f)][\Sigma(f)][V(f)]^H \tag{3}$$

Figure 4: Picking the peak singular value and corresponding mode shape vector, modified after [10]

where $\Sigma(f)$ is a diagonal matrix holding the singular values in descending order and $U(f)$ is a matrix holding the singular vectors. Dominating $s_1(f_i)$ peak indicates the presence of the i-th mode mode. $\{u_1(f_i)\}$ is a mode shape vector matching selected eigenfrequency [11]. Singular values corresponding to the singular vectors collinear with the singular vector of the peak singular value belong to the considered mode. Damping ratio can be obtained by taking the selected $s_1(f)$ to the time domain and calculating the logarithmic decrement of the decaying auto-correlation function [7].

3.2 Stochastic Subspace Identification

The SSI is a well-known component in system identification methods first introduced in [8] and [12] that combine a state-space realization models with different numerical techniques (QR and SV decompositions). In this work the modal parameters of the mast are assessed by the data driven SSI with unweighted principal component (SSI-UPC) included in the ARTeMIS software [10]. Herein the brief description of the general data driven SSI method is presented.

The behavior of structural system is modeled by the linear time-invariant equation of motion (4).

$$\begin{cases} M\ddot{u}(t) + C\dot{u}(t) + Ku(t) = f(t) \\ y(t) = B_a\ddot{u}(t) + e(t) \end{cases} \tag{4}$$

where M, C, K are the mass, damping and stiffness matrix, u represents the continuous time displacement vector and f denotes the external force which is not measured but represented as white noise. Vector y contains measured operational responses, in this case the accelerations, B_a is the output location matrix for the accelerometers used and e represents the measurement noise. The discrete time state-space formulation of (4) in a time step $k\tau$ is written as (5).

$$\begin{aligned} x_{k+1} &= A_d x_k + v_k \\ y_k &= C_d x_k + w_k \end{aligned} \tag{5}$$

where A_d is the discrete time state matrix describing the dynamics of the system and C_d is the output observation matrix. Vectors v_k and w_k denote the process and measurement noise. The idea in data driven SSI is to relate the response formulation from (5) to a transformation of block Hankel matrix H formulated based on y_k. The size of the block Hankel matrix yields $N - 2k$ columns and $2k$ block rows where N, k and m are the number of the data points, time shift and number of blocks respectively. The transformation is referred to as a projection of the split H matrix such as that $H_{[:,1:k]}$ block rows are projected on $H_{[:,k+1:2k]}$ resulting in a projection matrix O. When assuming that the matrix H contains a zero mean Gaussian signals, the projection is expressed as a conditional mean of the recorded random responses and the matrix O contains free decays of the system. Relation between the projection matrix and (5) is described in (6).

$$O = \begin{bmatrix} C_d \\ C_d A_d \\ C_d A_d{}^2 \\ \vdots \\ C_d A_d{}^{k-1} \end{bmatrix} X = \Gamma X \tag{6}$$

where Γ is the observability matrix and X is the matrix of initial conditions of the free decays [13]. The projection matrix can be truncated by using the SVD of the initial O and constructing the new matrix from the non-zero singular values, Σ_1 see (7). The observability matrix and the state vector are formulated by (8).

$$O = \begin{bmatrix} U_1 & U_2 \end{bmatrix} \begin{bmatrix} \Sigma_1 & 0 \\ 0 & \Sigma_2 \end{bmatrix} \begin{bmatrix} V_1{}^T \\ V_2{}^T \end{bmatrix} \tag{7}$$

$$\begin{aligned} \Gamma &= U_1 \Sigma_1{}^{0.5} \\ X &= \Sigma_1{}^{0.5} V_1{}^T \end{aligned} \tag{8}$$

Finally, the discrete time state matrix is found from the regression of Γ. The discrete time poles are obtained from the eigenvalue decomposition of A_d matrix, where the eigenvalues and the damping ratios are calculated by the classical modal analysis formulas like in [11].

4 Data Interpretation

This section presents the overview of data gathered during the measurement period of $09/2013 - 12/2013$. First, a general overview of the measurements is presented. The modal properties of the mast are obtained by EFFD routines programmed in MATLAB and SSI-UPC techniques in ARTeMIS [10]. Section ends with separation of the system damping components using best-practice from the standards [4] and the existing knowledge regarding the MB foundation [6].

4.1 Measurement description

In total 50 days of the continuous measurements is sampled with the frequency of $20\,\mathrm{Hz}$ and analyzed. During that period the structure experienced several significant storms including hurricane winds of *Christian* and *Bodil* [14].

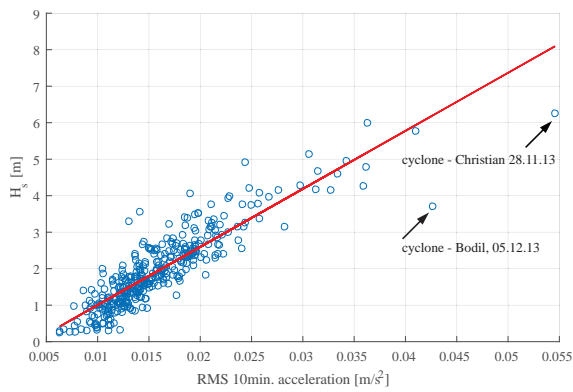The structural responses illustrated in Figure 5 are in good correlation with the significant wave heights (H_s).

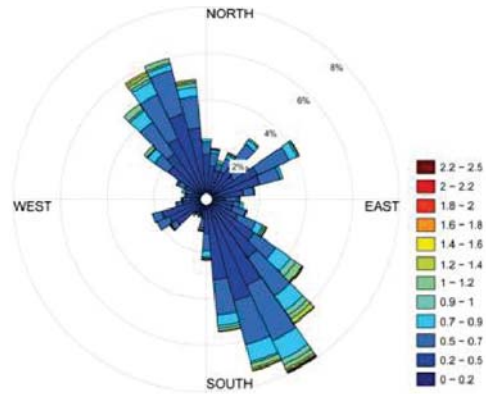Figure 5: The correlation of the RMS acceleration with the H_s through the measurement period.

Figure 6: The acceleration response rose through the measurement campaign, $\frac{m}{s^2}$.

The structural monitoring system is not equipped with anemometer however two samples with the highest error in the Figure 5 indicate the presence of strong wind events. The design basis for the location states that the main wave load direction is N-W which is in good agreement with the rose obtained from the accelerometers, see Figure 6. The S-W is the main direction of the wind load what is also visible in Figure 6. Based on both Figure 5 and 6 it can be clearly stated that the response of the structure is driven by the wave loads, which will be correlated to the modal parameters in the next sections.

4.2 Ambient vibration analysis

Raw accelerometer data is detrended and high-pass filtered with the frequency cut-off of 0.01 Hz. For OMA accelerations were divided into 100 clusters reflecting a similar loading conditions with the long lengths varying from 2-12 h. The singular values of PSD for a single event are presented in Figure 7. The singular values for the measurement campaign are illustrated in Figure 8.
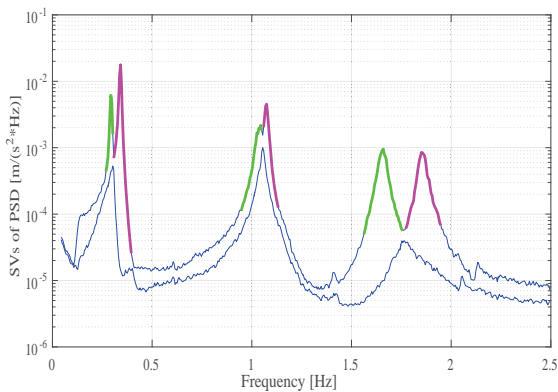

Figure 7: The singular values of the PSD matrix of the accelerations with the highlighted modes.
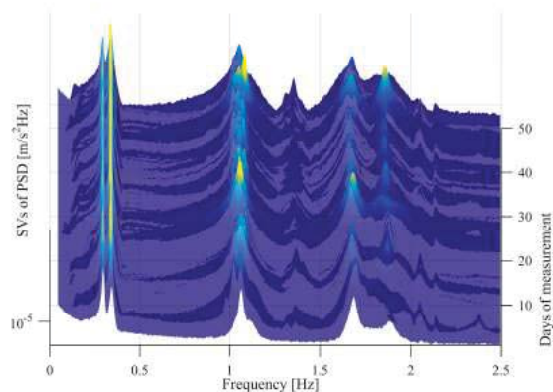

Figure 8: The singular values of the PSD matrices of the accelerations.

The 3 sets of the 2 orthogonal closely spaced bending modes can be identified in the frequency range of 0.01-2.5 Hz Figure 7. The singular values representing auto PSD for each mode are highlighted in green and purple for the each set in Figure 7. Figure 8 illustrates that the eigenfrequency of all the modes remain constant throughout the measurement period. The frequent appearance of a torsional mode in the vicinity of 1.4 Hz is correlated with the wider 1st singular values spectrum that is proportional to the calculated H_s.
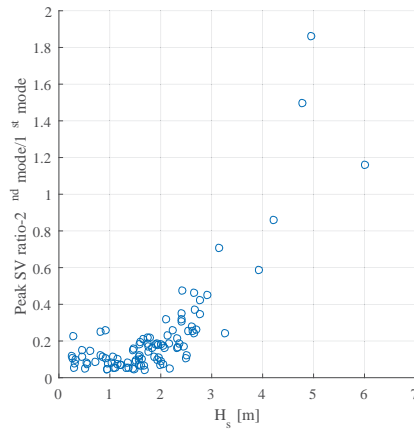
Figure 9: The ratio between the peak SV of the 2nd and the 1st mode.

Figure 9 illustrates the ratio between the mean of the singular values for the first and second mode correlated with the H_s. Assuming that the left and right singular vectors in (2) are not subjected to any change through the measurement period, then the magnitude of the peak singular values (highlighted green and purple for the 2 sets of modes at the $0.34\,\text{Hz}$ and $1.01\,\text{Hz}$ in the Figure 7) is changing only due to the loading conditions. For the calm sea the first mode response is dominant. With the increasing wave heights the second mode is more significant, reaching half the magnitude of the 1st mode for the typical fatigue wave height in the North Sea, [2], and doubled the contribution for the storm events. In practice this result illustrate that for load calculations like those presented in [2], the second mode shape should be accounted for in the response of the mast in order not to underestimate the load.

The eigenfrequencies and damping ratios of the 1st mode are estimated using the SSI-UPC and EFDD techniques. The comparison of the two techniques with correlation to the H_s and the histogram of system damping estimated using SSI-UPC are presented in Figures 10, 11 and 12.
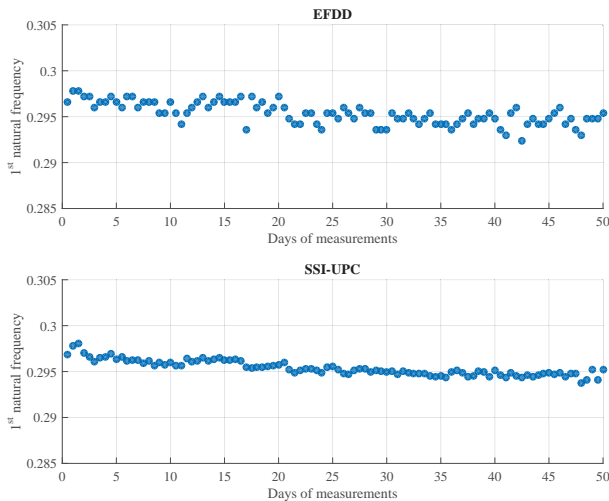

Figure 10: The eigenfrequency the 1st mode for the measurement period. Comparison between the EFDD and SSI-UPC techniques.
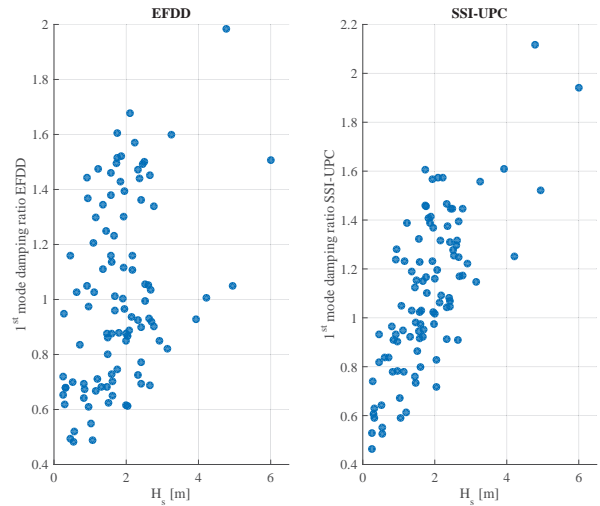
Figure 11: The correlation of the 1st mode damping ratios and H_s for the measurement period. Comparison between the EFDD and SSI-UPC techniques.

Regarding the 1st mode eigenfrequency, the result obtained from both methods agree very well and identify

the frequency close to 0.295 Hz throughout the measurements. By the visual inspection, the EFDD results are more scattered than the SSI-UPC however the mean error between EFDD and SSI-UPC is 0.2% with the standard deviation of 0.16%.

According to Figure 11, the results obtained from both techniques illustrate the linear correlation between the 1st mode damping ratio and the H_s. The maximum added offshore damping ratios in the range of 2% is reached for the two storm events where the highest acceleration measurements peaks at $1.8\frac{m}{s^2}$. The minimum damping of 0.45% is observed during the calm sea states and the accelerations of $0.03\frac{m}{s^2}$.

The histogram presented in Figure 12 illustrates that the damping ratio of the 1st mode is close to be normally distributed over the measurement campaign, with a 5% quantile and a 95% quantile of 0.57% and 1.61% respectively.
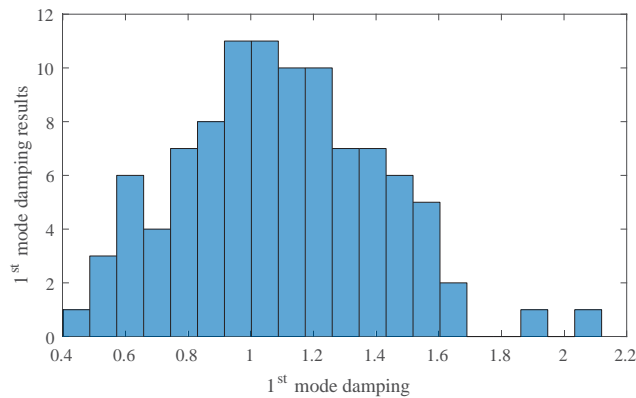

Figure 12: The histogram of the 1st mode damping ratio throughout the measurement campaign.

Having analyzed the general behavior of the 1st mode damping of the mast, the separation of its main components is addressed.

The minimum estimated system damping is equal to 0.45%, see Figure 11. Based on [4] the viscous hydrodynamic damping component for the relative velocities during the calm sea is negligible. The radiation part of the hydrodynamic damping for the cylindrical structure of the 1st natural frequency close to the 0.3 Hz is equal to 0.12% [4]. When subtracted the structural damping stated in [4] the soil damping contribution in the minimum system damping is 0.05-0.15%.

The maximum damping estimated for the storm conditions is equal to 2.1%, see Figure 11. Based on the soil damping-acceleration correlation for the MB in sand presented in [6], the soil damping for measured acceleration levels oscillates at 0.6-0.8%. By subtracting the latter and accounting for the structural damping, the hydrodynamic damping contribution to the system damping during the storm event would oscillate in the range of 0.9-1.2%.

5   Conclusion

This paper presents an experimental study of the long-term dynamic properties of the meteorological mast supported by the Mono Bucket foundation using the OMA methods. Based on the results and supported with the existing knowledge the paper addresses the contributions of the hydrodynamic, soil and structural damping to the added offshore damping. Linear correlation between the system damping and the wave heights measured on the site is obtained, with a substantial contribution of the hydrodynamic damping component during the storm events. The results expands the knowledge about the new foundation concept and can find use in the fatigue limit state calculations.

The future work will consider comparison between the experimental data with a numerical boundary element model of soil and foundation.

References

[1] G.T. Houlsby, B.W. Byrne, *Suction Caisson Foundations for Offshore Wind Turbines and Anemometer Masts*, Wind Engineering 24(2000), pp. 249-255

[2] M. Seidel, *Wave induced fatigue loads*, Stahlbau, 83 (2014), pp. 535-541

[3] D.J. Cerda Salzmann, J. van der Tempel, *Aerodynamic damping in the design of support structures for offshore wind turbines*, *Proceedings Copenhagen Offshore Conference*, Copenhagen, Denmark, 2005

[4] P. Gujer, *Overall Damping for Piled Offshore Support Structures*, GL RC Guideline for the Certification of Offshore Wind Turbines, Edition 2005

[5] N.J. Tarp-Johansen, L. Andersen, E.D. Christensen, C. Mϕrch, B. Kallesϕe, S Frandsen, *Comparing Sources of Damping of Cross-Wind Motion*, *European Offshore Wind 2009: Conference & Exhibition*, The European Wind Energy Association, 2009

[6] M. Damgaard, *Dynamic Properties of Offshore Wind Turbine Foundations*, Aalborg University, Department of Civil Engineering, 2014

[7] R. Brincker, L. Zhang, P. Andersen, *Modal Identification from ambient responses using frequency domain decomposition*, *Proceedings of the International Modal Analysis Conference (IMAC)*, San Antonio, Texas, USA, 2000. pp. 625-630.

[8] P. Overschee, B. De Moor, *Subspace Identification for Linear Systems*, Boston, MA: Springer US, 1996.

[9] J.S. Bendat, A.G. Piersol, *Random data: Analysis and measurement procedures. 4th edn* United Kingdom: Wiley-Blackwell, 2010

[10] P. Andersen, *ARTeMIS Modal 4.4- User Manual* Structural Vibration Solutions A/S

[11] R. Brincker, C. Ventura, *Introduction to operational modal analysis* United States: John Wiley & Sons, 2015

[12] B.L Ho, R.E. Kalman, *Effective construction of linear state-variable models from input/output data.* Regelungstechnik 14 (1966), pp. 545-548

[13] R. Brincker, P. Andersen, *Understanding Stochastic Subspace Identification*, *IMAC-XXIV : A Conference & Exposition on Structural Dynamics*, 2006

[14] *Bodil Klassificeret Som 'Orkanlignende' (in danish): DMI* http://www.dmi.dk. N.p., 2016. Web. 11 May 2016.